**UKAEA FUS 429**

**EURATOM/UKAEA Fusion**

# The effects of sheared toroidal plasma rotation on the internal kink mode in the banana regime

J P Graves, R J Hastie and K I Hopcraft

May 2000



EURATOM/UKAEA Fusion Association

Culham Science Centre, Abingdon
Oxfordshire, OX14 3DB
United Kingdom
Telephone +44 1235 463532
Facsimile +44 1235 463647

# The Effects of Sheared Toroidal Plasma Rotation on the Internal Kink Mode in the Banana Regime

J P Graves[1,2], R J Hastie[2,3] and K I Hopcraft[1]

[1]School of Mathematical Sciences, University of Nottingham, University Park, Nottingham, NG7 2RD, UK

[2]EURATOM/UKAEA Fusion Association, Culham Science Centre, Abingdon, Oxfordshire, OX14 3DB, UK

[3]Current Address: MIT Plasma Science and Fusion Center, 167 Albany Street, NW16-234 Cambridge, MA 02139, USA

**Abstract.** The stability of the ideal internal kink mode is calculated, taking into account the kinetic response of thermal ions in the external region and the singular layer. By extending the collisionless dispersion relation to include the equilibrium radial electric field it is found that the stability of the internal kink mode depends sensitively on sheared toroidal plasma rotation. The sheared toroidal plasma rotation can increase the critical pressure for internal kink mode displacements by a factor typically of two.

## 1. Introduction

In this paper we consider the question of extended sawtooth quiescent periods in present and future tokamak experiments, and the possible relationship to strong kinetic stabilisation. A particularly relevant issue addressed here is the effect that the equilibrium radial electric field and toroidal plasma rotation may have on sawteeth. This appears to be a somewhat neglected area of research, even though in many experiments the plasma rotation frequency is observed to be large.

In recent years, interest has focused on the kinetic effects arising from collisionless energetic populations of ions (as distinct from thermal ions) on the internal kink mode. The theoretical interpretations of kinetic effects on fishbones [1] and sawteeth [2] have been particularly successful. For the case of fishbones, the instability has been identified with a mode satisfying $\omega \sim \langle\omega_{mdh}\rangle$ [3], where $\omega$ is the normal mode frequency and $\langle\omega_{mdh}\rangle$ is the magnetic drift frequency of hot minority ions averaged over trapped particle orbits (denoted by angular brackets '<>'). Kinetic effects enter the analysis through an additional term which generalises the minimised MHD fluid potential energy calculated for example by Bussac *et al* [4]; these are often found to be strongly destabilising for regimes corresponding to neutral beam injection (NBI) heated plasmas. Furthermore, the success of ion cyclotron resonance heating (ICRH) in controlling sawtooth activity at JET [5] has also been interpreted using the generalised potential energy. Comparisons between theory and experiment are fruitful, with particularly strong correlations between JET DTE1 sawtoothing discharges and kinetic stabilisation reported recently in Refs. [6, 7].

In sufficiently hot plasmas thermal ions also give rise to significant kinetic effects [8, 9], and an unstable mode has been identified with $\omega \sim \langle\omega_{mdi}\rangle$, where $\langle\omega_{mdi}\rangle$ is the bounce averaged magnetic drift frequency of trapped thermal ions. However, in many experiments the toroidal plasma rotation $\Omega_\Phi(r)$ caused by the equilibrium radial electric field is at least as large as $\langle\omega_{mdi}\rangle$, and to interpret the kinetic effects of such plasmas on sawteeth the potential energy term should be generalised to include the effects of a finite equilibrium electric field. Furthermore, by including these additional effects, it will be shown that the internal kink mode is sensitive to the magnitude and profile of $\Omega_\Phi(r)$. For some regimes the kinetic effects of thermal ions can be stabilising, as is found for ICRH minority ions. However, for a sufficient change in the amplitude, or indeed profile of $\Omega_\Phi(r)$, the kinetic effects can be destabilising. In addition it is shown that if the plasma rotation profile is not sheared, the effects of finite $\Omega_\Phi$ on stability disappear. In this paper $\Omega_\Phi$ is limited to an ordering $\Omega_\Phi \sim \omega_{*pi}$, with $\omega_{*pi}$ the diamagnetic frequency of thermal ions. This analysis therefore differs from previous work which has concentrated on the effects of sheared toroidal plasma rotation in the sonic range on the ideal MHD internal kink mode [10].

Many experimental observations suggest a link between sawtooth activity and plasma rotation. For example, in locked mode experiments a change in the $m = 2$, $n = 1$ resonant magnetic perturbation amplitude and a corresponding change in the

amplitude and shear of $\Omega_\Phi$ can remove sawteeth altogether [11]. Moreover, in NBI experiments, a reversal in the direction of the minority ion injection, and corresponding plasma rotation direction, can significantly modify the sawtooth period and amplitude.

In this paper, the impact of toroidal plasma rotation is analysed chiefly via evaluation of the critical poloidal beta for instability, where the poloidal beta is defined by

$$\beta_p = -\frac{2\mu_0}{B_0^2 \epsilon_1^2 r_1^2} \int_0^{r_1} r^2 \frac{dP}{dr} dr. \tag{1}$$

In Eq. (1), $\mu_0$ is the relative permeability of free space, $B_0$ the axial magnetic field strength, $r$ the minor radius and $r_1$ the radial location of the singular layer with $q(r_1) = 1$, $q$ is the safety factor, $\epsilon_1 = r_1/R_0$ is the inverse aspect ratio with $R_0$ the major radius of the tokamak, and $P$ the plasma pressure. The ideal internal kink mode is stable when $\beta_p < \beta_p^c$, a critical value, and this classical measure of the internal kink stability [4] is chosen for two principal reasons. First, it provides useful information regarding the ideal stability threshold. Indeed, the MHD critical value $\beta_p^c$ provides a benchmark with which to gauge modifications that correspond to the kinetic effects of the thermal ions. Second, evaluating $\beta_p^c$ only requires solving the internal kink mode dispersion relation at marginal stability: while retaining a finite mode oscillation frequency, the kinetic terms are greatly simplified for cases where the growth rate is zero, and thus allow the kinetic potential energy of the thermal ions and the dispersion relation to be solved exactly.

The paper is organised as follows. Section 2 describes the relative sizes of various competing natural frequencies and provides an analysis that extends the kinetic internal kink mode dispersion relation to include the equilibrium radial electric field and induced plasma rotation. In Section 3 the typical characteristics (including the plasma rotation magnitude and profile) of sawtoothing discharges are described, and represented in a model that is subsequently used to assess the effect of plasma rotation on the internal kink mode. Quantitative results based on the theoretical extensions and models of Sections 2 and 3 are contained in Section 4. Finally, the results of this paper are summarized, and the implications for fusion research are discussed in Section 5. Technical details pertaining to the kinetic treatment of the singular layer are assigned to the Appendix.

## 2. Internal Kink Mode Dispersion Relation for Toroidally Rotating Plasmas

In this section the ideal internal kink mode dispersion relation is extended to include the effects of finite toroidal plasma rotation. Before this can be done, the magnitude of the various frequencies that appear in the dispersion relation must be considered. Including an equilibrium radial electrostatic field in the equation of motion and assuming that poloidal flows are strongly damped [12], the toroidal rotation frequency is given by:

$$\Omega = \Omega_\Phi + \omega_{*pi} \tag{2}$$

with

$$\Omega_\Phi = -\frac{q\Phi'}{B_0 r} \text{ and } \omega_{*pi} = -\frac{qP_i'}{eZn_iB_0r}. \tag{3}$$

Here $eZ$, $n_i$, $P_i$ are, respectively, the ion charge, ion density and ion pressure and $\Phi$ is the electrostatic potential, so that the radial equilibrium electric field is $E_r = -\Phi'$, where $' \equiv \partial/\partial r$. The frequencies $\Omega_\Phi$ and $\omega_{*pi}$ have the same sign provided the equilibrium electric field is positive; the electrostatic and diamagnetic contributions are in opposition if the electric field is negative.

In most of the regimes examined in the following sections it is found that the solution to the dispersion relation satisfies $\Re\{\omega\} \equiv \omega_r \sim \omega_{*pi}$, and, in addition, in modern large hot tokamaks the thermal ion temperatures are sufficiently high to ensure that whilst $\omega_{*pi}$ is large, the effective collision frequency of trapped thermal ions $\nu^i_{\text{eff}}$ is, by comparison, relatively small, ie $\nu^i_{\text{eff}}/\omega_{*pi} \ll 1$, thereby justifying the collisionless limit. Throughout this paper the collisionless limit is assumed. This assists in reducing the number of parameters appearing in the theory and clarifies the origin of the various trends observed in the results. Also, because the effective electron collision frequency is large ($\nu^e_{\text{eff}}/\nu^i_{\text{eff}} = \sqrt{m_i/m_e}$, where $m_i/m_e$ is the ion-electron mass ratio), electrons do not contribute significantly to kinetic behaviour, unlike thermal ions.

The plasma rotation is limited to $\Omega_\Phi \sim \omega_{*pi}$, or equivalently, $E_r \sim \partial P_i/\partial r \,/\, n_i eZ$. Such an ordering simplifies the formalism describing internal kink mode stability. This follows from the fact that MHD fluid terms do not depend directly on the diamagnetic component of the plasma rotation because $\omega_{*pi}$ is small. As a result the MHD fluid terms are also independent of $\Omega_\Phi \sim \omega_{*pi}$. Even at higher velocities where centrifugal effects are taken into account only small modifications to the MHD stability have been calculated [10]. For kinetic terms, the situation is markedly different. Here it is found that the dynamics of single particles are strongly modified by the radial electric field. In particular, an electric field dominates over inhomogeneous magnetic field effects on trapped precessing particles. Since kinetic terms describe single particle and collective resonances, perturbations of a kinetic origin are also strongly modified by an electrostatic potential. If no such potential exists the dynamics is simplified and the perturbed kinetic distribution function defined in Ref. [3] applies in the external region. In this paper the effects of finite $\Omega_\Phi$ on the fluid and kinetic terms of the singular layer are also taken into account.

It is useful to review the form of the perturbed thermal ion distribution function for the external region when $\Omega_\Phi = 0$ [13]:

$$\delta f_i = -\boldsymbol{\xi}\cdot\boldsymbol{\nabla} f_i + 2\,\frac{\omega - n\frac{m_i}{Ze}\frac{\partial f_i/\partial\psi|_{\mathcal{E}}}{\partial f_i/\partial\mathcal{E}|_\psi}}{\omega - n\frac{m_i}{Ze}\frac{\partial \mathcal{J}/\partial\psi|_{\mathcal{E}}}{\partial \mathcal{J}/\partial\mathcal{E}|_\psi}}\;\left.\frac{\partial f_i}{\partial\mathcal{E}}\right|_\psi \mathcal{E}\,\langle J\rangle\,. \tag{4}$$

Here $f_i$ is the equilibrium thermal ion distribution function, $\mathcal{E} = v^2/2$, $\boldsymbol{\xi}$ the fluid displacement, $\mathcal{J}$ the longitudinal invariant, so that $J = \lambda B\boldsymbol{\nabla}\cdot\boldsymbol{\xi}_\perp/2 - \boldsymbol{\xi}_\perp\cdot\boldsymbol{\kappa}(1-3\lambda B/2)$, where $\lambda = \mu/\mathcal{E}$ with $\mu = v_\perp^2/2B$ the magnetic moment and $\boldsymbol{\kappa}$ is the magnetic field line curvature vector, $n$ is the toroidal mode number and $\psi$ is the magnetic flux where, for

circular flux surfaces, $r\,B_0\,dr = q(r)\,d\psi$. Inspecting the RHS of Eq. (4), the first term is the convective component, which gives rise to fluid MHD quantities, and the second term is the perpendicular compressional term, giving kinetic effects. Kinetic quantities can be recognised through the frequencies

$$\omega_{*i} = \frac{m_i}{Ze}\frac{\partial f_i/\partial\psi\,|_{\mathcal{E}}}{\partial f_i/\partial\mathcal{E}\,|_{\psi}} \quad \text{and} \quad \langle\omega_{mdi}\rangle = \frac{m_i}{Ze}\frac{\partial\mathcal{J}/\partial\psi\,|_{\mathcal{E}}}{\partial\mathcal{J}/\partial\mathcal{E}\,|_{\psi}}. \tag{5}$$

The numerator of Eq. (4) contains the difference between the internal kink mode frequency and the ion diamagnetic frequency. The denominator contains the difference between the kink mode frequency and the magnetic precessional frequency of trapped thermal ions.

We now turn to the more general scenario where there is an equilibrium radial electric field and examine how this modifies the resonances appearing in Eq. (4). Unperturbed particles now have

$$\mathcal{K} = \mathcal{E} + Ze\Phi/m_i \tag{6}$$

as a constant of their equilibrium motion. Antonsen and Lee [13] developed a drift-kinetic equation in terms of $\mathcal{K}$, and the adiabatic invariants $\mu$ and $\mathcal{J}$, and solved it for the perturbed $\delta f_i$. Following Ref. [13], the only changes to Eq. (4) that result from the inclusion of a non-zero equilibrium electrostatic potential correspond to the transformations $\partial/\partial\mathcal{E}\,|_{\psi} \longrightarrow \partial/\partial\mathcal{K}\,|_{\psi}$ and $\partial/\partial\psi\,|_{\mathcal{E}} \longrightarrow \partial/\partial\psi\,|_{\mathcal{K}}$. Hence Eq. (4) is generalised to

$$\delta f_i = -\boldsymbol{\xi}\cdot\nabla f_i + 2\,\frac{\omega - n\frac{m_i}{Ze}\frac{\partial f_i/\partial\psi|_{\mathcal{K}}}{\partial f_i/\partial\mathcal{K}|_{\psi}}}{\omega - n\frac{m_i}{Ze}\frac{\partial\mathcal{J}/\partial\psi|_{\mathcal{K}}}{\partial\mathcal{J}/\partial\mathcal{K}|_{\psi}}}\,\left.\frac{\partial f_i}{\partial\mathcal{K}}\right|_{\psi}\mathcal{E}\,\langle J\rangle\,. \tag{7}$$

Whilst the kinetic component of the perturbed distribution function is modified, the fluid component is unchanged.

We now explore in more detail how the equilibrium electric field affects the kinetic component of the perturbed distribution function $\delta f_i$ and relate these changes to the equilibrium plasma rotation $\Omega_\Phi$. Regardless of whether $\Phi$ is non-zero, the longitudinal invariant

$$\mathcal{J} = \oint v_{\|}dl,$$

with the integration between trapped particle bounce points, is conserved and in general one can define the drift precession frequency [14] as:

$$\langle\omega_{di}\rangle = \frac{m_i}{Ze}\frac{\partial\mathcal{J}/\partial\psi\,|_{\mathcal{K}}}{\partial\mathcal{J}/\partial\mathcal{K}\,|_{\psi}}. \tag{8}$$

To evaluate expression (8) it is necessary to define the parallel velocity in terms of $\mathcal{K}$ rather than $\mathcal{E}$: $v_{\|} = \sqrt{2}\,(\mathcal{K} - \mu B - eZ\Phi/m_i)^{1/2}$, giving

$$\left.\frac{\partial\mathcal{J}}{\partial\psi}\right|_{\mathcal{K}} = \oint\left(\frac{Rv_{\|}}{q}\frac{\partial q}{\partial\psi} - \frac{\mu}{v_{\|}}\frac{\partial B}{\partial\psi}\right)dl - \frac{eZ}{m_i}\frac{\partial\Phi}{\partial\psi}\oint\frac{dl}{v_{\|}} \quad \text{and} \quad \left.\frac{\partial\mathcal{J}}{\partial\mathcal{K}}\right|_{\psi} = \oint\frac{dl}{v_{\|}}.$$

The first and second terms appearing in the first integral correspond to the curvature drift and $\nabla B$ drift respectively and collectively identify the magnetic drift. The second integral corresponds to the drift due to the electric field. Using $r\,B_0\,dr = q(r)\,d\psi$ and referring to Eq. (3) yields:

$$\langle \omega_{di} \rangle \equiv \frac{m_i}{Ze} \frac{\partial \mathcal{J}/\partial \psi \mid_{\mathcal{K}}}{\partial \mathcal{J}/\partial \mathcal{K} \mid_{\psi}} = \langle \omega_{mdi} \rangle + \Omega_\Phi . \tag{9}$$

Thus an equilibrium electric field modifies the bounce averaged drift frequency of trapped ions in exactly the same way as it does the bulk toroidal plasma rotation $\Omega$.

The remaining quantity occurring in the numerator of Eq. (7) requires evaluation. For this application the Maxwellian distribution written in terms of $\mathcal{K}$ is required:

$$f_i = n_i \left( \frac{m_i}{2\pi T_i} \right)^{3/2} \exp\left( \frac{Ze\Phi}{T_i} \right) \exp\left( \frac{-m_i \mathcal{K}}{T_i} \right) . \tag{10}$$

Using Eqs. (5) and (3) it can be seen that

$$\frac{m_i}{eZ} \frac{\partial f_i/\partial \psi \mid_{\mathcal{K}}}{\partial f_i/\partial \mathcal{K} \mid_{\psi}} = \omega_{*i} + \Omega_\Phi . \tag{11}$$

It is now possible to identify the modifications of the perturbed kinetic distribution function which are attributable to finite $\Omega_\Phi$. Using Eqs. (9) and (11) and noting $\partial f_i(r,\mathcal{E})/\partial \mathcal{E} \mid_r = \partial f_i(r,\mathcal{K})/\partial \mathcal{K} \mid_r$ when $f_i$ is Maxwellian, the kinetic contribution to Eq. (7) becomes

$$\delta f_{ki} = 2 \left( \frac{\omega - \Omega_\Phi(r) - \omega_{*i}}{\omega - \Omega_\Phi(r) - \langle \omega_{mdi} \rangle} \right) \frac{\partial f_i}{\partial \mathcal{E}} \mathcal{E} \langle J \rangle , \tag{12}$$

on setting $n = 1$. Comparing Eq. (12) with the kinetic contribution to Eq. (4) it is clear that the inclusion of finite $\Phi$ has the effects $\omega_{*i} \to \omega_{*i} + \Omega_\Phi$ and $\omega_{mdi} \to \omega_{mdi} + \Omega_\Phi$. This transformation applies throughout the analysis, and $\delta W_{ki}$ can be obtained by following the method of Ref. [3] on replacing the kinetic component of Eq. (4) with the generalised term of Eq. (12).

We now consider the singular layer and more generally the internal kink dispersion relation. Matching the layer solution for $\boldsymbol{\xi}$ to the ideal regions $r < r_1$ and $r > r_1$ yields the following dispersion relation [15, 16]:

$$\frac{\gamma_I}{\omega_A} \frac{s\sqrt{1+\Delta}}{3\pi} \frac{1}{\varepsilon^2} \bigg|_{r_1} = -\delta \hat{W} , \tag{13}$$

where the magnetic shear $s = rq'/q$, $\omega_A = v_A/R_0$ with $v_A$ the Alfvén velocity, $\varepsilon = r/R_0$, $\delta W = \delta \hat{W}\, 6\pi^2 \xi_0^2\, R_0 B_0^2 \varepsilon_1^4/\mu_0$, $\gamma_I^2 = -\omega(\omega - \omega_{*pi})|_{r_1}$ and $\Delta = 2q^2$ [17].

Finite $\Omega_\Phi$ effects are introduced by noting that the inertia is most conveniently calculated in the absence of an electrostatic potential. This can be arranged by transforming the eigenvalue $\omega$ to a frame moving with the toroidal rotation at the resonant surface $\Omega_\Phi(r_1)$, i.e. $\omega \to \omega - \Omega_\Phi(r_1)$, thus giving [15, 18]:

$$\gamma_I^2 = -(\omega - \Omega_\Phi)(\omega - \omega_{*pi} - \Omega_\Phi)|_{r_1} . \tag{14}$$

To be consistent with the external region, collisionless kinetic effects of thermal ions are retained in the singular layer. Following a procedure similar to that of Ref. [19], plasmas in the banana regime have the above definition of $\Delta$ modified to [7]:

$$\Delta = \frac{1.6q^2}{\varepsilon_1^{1/2}}\left[1 + O(\varepsilon_1^{1/2})\right],$$

Details regarding the evaluation of $\Delta$ can be found in the Appendix.

From Eqs. (13) and (14), the generalised ideal internal kink mode dispersion relation is :

$$D(\tilde{\omega}) = -i\left.\frac{\sqrt{\tilde{\omega}(\tilde{\omega}-\omega_{*pi})}}{\omega_A}\right|_{r_1} + \varepsilon_1^2\frac{3\pi}{s_1\sqrt{1+\Delta}}\left[\delta\hat{W}_f + \delta\hat{W}_{ki}(\tilde{\omega})\right] = 0, \quad (15)$$

where the Doppler shifted eigenfrequency is

$$\tilde{\omega} = \omega - \Omega_\Phi(r_1). \quad (16)$$

Substituting Eq. (4) for the kinetic component of Eq. (12) yields [3]:

$$\delta W_{ki}(\tilde{\omega}) = -2^{7/2}\pi^3 m_i\left(\frac{\xi_0}{R_0}\right)^2\int_0^{r_1} dr\, r^2\int_0^1 dk^2\,\frac{I_q^2}{K_b}$$
$$\times\int_0^\infty d\mathcal{E}\,\mathcal{E}^{5/2}\frac{\partial f_i}{\partial\mathcal{E}}\left[\frac{\tilde{\omega}-[\omega_{*i}+\Omega_\Phi(r)-\Omega_\Phi(r_1)]}{\tilde{\omega}-[\langle\omega_{mdi}\rangle+\Omega_\Phi(r)-\Omega_\Phi(r_1)]}\right], \quad (17)$$

where $k^2 = [1+\lambda B_0(\varepsilon-1)]/(2\varepsilon\lambda B_0)$,

$$K_b(k^2) = \frac{1}{\pi}\sqrt{\frac{2}{\varepsilon}}K(k^2)\,,\; I_q(r,k^2) = \frac{1}{\pi}\sqrt{\frac{2}{\varepsilon}}\int_0^{\frac{\pi}{2}}\frac{\cos[2q\sin^{-1}(\sqrt{k^2}\sin\phi)]}{\sqrt{1-k^2\sin^2\phi}}d\phi, \quad (18)$$

and $K(k^2)$ is a complete elliptic integral of the first kind [20].

In Section 4 the above generalised dispersion relation is solved numerically for various regimes inferred from the models and parameters described in Section 3. For the present it is of interest to emphasise some of the more obvious characteristics regarding the generalised dispersion relation. Consider $\Omega_\Phi(r) - \Omega_\Phi(r_1) \gg \tilde{\omega}$. If $\Omega_\Phi(r) - \Omega_\Phi(r_1)$ is large enough, the square bracket of Eq. (17) will approach unity and consequently $\delta\hat{W}_{ki}$ will be independent of $\Omega_\Phi$, $\tilde{\omega}$, $\omega_{*pi}$ and $\langle\omega_{mdi}\rangle$. This result is identical to the Kruskal and Oberman limit [21] of $\tilde{\omega}\to\infty$, which yields the stability criterion

$$(\delta\hat{W}_0 - \delta\hat{W}_1\beta_p - \delta\hat{W}_2\beta_p^2) + \frac{\mu_1\sqrt{2\epsilon_1}}{8\pi\epsilon_1^2}\beta_i > 0 \quad (19)$$

where the $\delta\hat{W}_n$ terms depend only on the safety factor profile, $q(r)$, and are evaluated by Bussac et al [4]. Also $\mu_1 \approx 1.1$ (see Ref. [8]), which together with

$$\beta_i = \frac{5\mu_0}{2r_1^{5/2}}\int_0^{r_1} dr r^{3/2}\frac{2P_i}{B_0^2}, \quad (20)$$

contains the stabilising effect of trapped ion compression.

Now consider when the magnitude of $\Omega_\Phi$ is comparable with $\tilde{\omega}$, $\omega_{*pi}$ and $\langle\omega_{mdi}\rangle$, but the radial profile of $\Omega_\Phi$ is not sheared, i.e. $\Omega_\Phi(r) = \Omega_\Phi(r_1)$. It can be seen by inspection

of Eq. (17) that if $\Omega_\Phi$ is not sheared, the dispersion relation $D(\tilde{\omega})$ is independent of $\Omega_\Phi$. This result is intuitively obvious, since $\omega = \tilde{\omega} + \Omega_\Phi(r_1)$ represents the translation of a frame of reference rigidly moving relative to the laboratory frame.

In general however $\Omega_\Phi$ may be sheared. Experimentally it is found that $\Omega_\Phi$ is peaked at the plasma centre and decreases towards the plasma edge. For such an equilibrium it can be seen from Eq. (17) that $\delta W_{ki}(\tilde{\omega})$, and hence $D(\tilde{\omega})$, are sensitive to small changes in $\Omega_\Phi$, particularly for the most interesting regimes in which $\tilde{\omega} \sim \omega_{*pi} \sim \langle \omega_{mdi} \rangle \sim \Omega_\Phi$.

The reason why the dispersion relation is sensitive to sheared toroidal plasma rotation is because single particles are strongly affected by the equilibrium electric field. This is reflected in the local dependence of $\delta W_{ki}$ on $\Omega_\Phi(r)$ in both the numerator and denominator of the integrand in Eq. (17).

The inertia is affected by $\Omega_\Phi$ only through contributions to the dispersion relation from the singular layer. The Doppler shift observed in $\gamma_I$ corresponds to the equilibrium electric field at $r_1$. Therefore, since part of the dispersion relation contains an integral which is a function of $\Omega_\Phi(r)$ and another part which is a function of $\Omega_\Phi(r_1)$, sheared toroidal plasma rotation necessarily introduces non-trivial modifications to the stability of the internal kink mode in the banana regime.

## 3. Modelling the Effects of Plasma Rotation on Stability

This section describes the models and choice of parameters that will be used to obtain the solutions to the dispersion relation in Section 4. A convenient way to reduce the parameter space is to determine internal kink stability close to marginal threshold conditions.

At marginal stability, Eq. (15) can describe two different types of mode. One of these is in the Alfvén continuum, which requires either $\tilde{\omega} > \omega_{*pi}(r_1)$ or $\tilde{\omega} < 0$. Assuming this to be the case, the imaginary and real parts of Eq. (15), respectively, are

$$\left. \frac{s\sqrt{1+\Delta}}{3\pi\varepsilon^2} \frac{\sqrt{\tilde{\omega}(\tilde{\omega}-\omega_{*pi})}}{\omega_A} \right|_{r_1} - \Im\left\{\delta\hat{W}_{ki}\right\} = 0 \tag{21}$$

$$\delta\hat{W}_f + \Re\left\{\delta\hat{W}_{ki}\right\} = 0. \tag{22}$$

Equation (21) describes a balance between Alfvén continuum damping and the ion Landau drive. In this respect, when the frequency of the marginally stable mode lies in the continuum the mode resembles the fishbone instability discussed by Chen *et al* [3]. The other class of mode can be referred to as a 'gap mode' which experiences no continuum damping, since its frequency lies in the low frequency diamagnetic gap in the Alfvén continuum $0 < \tilde{\omega} < \omega_{*pi}(r_1)$. If the mode frequency, at marginal stability, falls within the diamagnetic gap then the mode is neither continuum nor Landau damped. Hence for $0 < \tilde{\omega} < \omega_{*pi}(r_1)$, the imaginary and real parts of Eq. (15) yield:

$$\Im\left\{\delta\hat{W}_{ki}\right\} = 0 \tag{23}$$

$$\left.\frac{s\sqrt{1+\Delta}}{3\,\pi\,\varepsilon^2}\,\frac{\sqrt{\tilde{\omega}(\omega_{*pi}-\tilde{\omega})}}{\omega_A}\right|_{r_1} + \delta\hat{W}_f + \Re\left\{\delta\hat{W}_{ki}\right\} = 0. \tag{24}$$

When the marginally stable mode is in the gap, finite Larmor radius effects provide additional internal kink stability through the positive definite inertial term in Eq. (24).

The stability of the internal kink mode is gauged by evaluating the critical poloidal beta $\beta_p^c$ at marginal stability. This quantity is chosen because the computation of $\beta_p^c$ permits direct comparison of the marginal stability boundary with the ideal MHD calculations of e.g. [4]. In evaluating the fluid potential energy $\delta\hat{W}_f$ we use the exact expression defined in Ref. [4], rather than approximate forms. However, a unique value for $\beta_p^c$ cannot be obtained from a dispersion relation that includes kinetic effects, since in addition to the pressure (and hence $\beta_p$), $\delta W_{ki}$ also depends on the temperature and density profiles. Thus $\beta_p^c$ depends on $\eta_i = d\ln T_i/d\ln n$, and $R/L_{T_i} = Rd\ln T_i/dr$; i.e on the two parameters which detemine stability of ion temperature gradient ( ITG ) modes. There is also a weak dependence on density because the inertial term scales as $\beta/n_i^{1/2}$. Throughout Section 4 $\beta_p^c$ is evaluated by keeping the central density $n_0$ fixed. Two pressure profiles (one more peaked than the other) are investigated and, within these, a range of values of $\eta_i$ is considered. Equal electron and ion pressures are assumed throughout. The problem is simplified by noting that when all frequencies are normalised to $\omega_{*pi}(r_1)$ both terms in Eq. (3.1) scale as $\beta_p$ (in the low beta limit where the trapped ion precessional drift does not depend on the equilibrium Shafranov shift of the magnetic surfaces or its radial variation). Thus, in the low beta limit, the imaginary part of the dispersion relation determines the mode frequency

$$\hat{\omega} \equiv \frac{\tilde{\omega}}{\omega_{*pi}(r_1)},$$

which can then be inserted into the real part of the dispersion relation to determine the critical value of $\beta_p$. At higher beta values, where the ion precessional drift depends on $\beta_p$ through the Shafranov shift (see below), a few iterations of this procedure converges to the required solution. This determines the values of $\beta_p$ and $\hat{\omega}$ at marginal stability. Perturbative analysis around these values is required to determine whether instability is predicted above or below the critical value $\beta_p^c$. This has been done, and establishes that the kink mode is unstable at higher values of $\beta_p$.

Considerable effort is made here to integrate $\delta W_{ki}$ without recourse to limiting approximations. Accurate representations of the pitch angle dependent quantities $I_q$ and $\langle\omega_{mdi}\rangle$ are required. For $I_q$ a two dimensional fit in $k^2$ and $q$ which accounts for the logarithmic singularity in pitch angle at the trapped-passing boundary $k^2 = 1$ is employed. It is accurate to within 0.01 percent for $0.5 < q < 1$ and $0 < k^2 < 1$. Writing

$$I_q = \frac{1}{\pi}\sqrt{\frac{2}{\varepsilon}}F_q(q,k^2),$$

the fit takes the form

$$F_q(q,k^2) \approx [2E(k^2) - K(k^2)] - \frac{4(1-q)\cos(\pi q)}{1-4(1-q)^2}[E(k^2) + (k^2-1)K(k^2)]$$

$$- \ (1+\cos(\pi q))f_1(q)\left[E(k^2)+(k^2-1)K(k^2)+\frac{2}{\pi}E(k^2)-1\right]$$
$$- \ (1+\cos(\pi q))[E(k^2)-K(k^2)]-f_2(q)(1-k^2)\left[\frac{\pi}{2}-K(k^2)\right] \quad (25)$$

with

$$f_1(q)=\frac{\pi}{2}\left[1.0841-0.3193(1-q)^2-0.0683(1-q)^4\right],$$
$$f_2(q)=5.1\left(q-\frac{1}{2}\right)(1-q)^2[1-0.034(1-q)],$$

and $E(k^2)$ a complete elliptic integral of the second kind [20].

For cases where $\beta = 2\mu_0 P/B_0^2$ is relatively large, the effects of Shafranov shifted circular flux surfaces on the magnetic drift of trapped ions [22] must be included. Unlike most other studies, where the effects of finite pressure on trapped ion orbits have been neglected, the definition of $\langle\omega_{mdi}\rangle$ used in the computations of Section 4 include finite $\beta$ effects. Referring to Connor *et al* [22]:

$$\langle\omega_{mdi}\rangle=\frac{qm_i\mathcal{E}}{eZB_0R_0r}\left[F_1+2sF_2-\alpha\left(\frac{1}{4q^2}+F_3\right)\right], \quad (26)$$

where $F_{1,2,3}$ are defined in terms of complete elliptic integrals of the first and second kind:

$$F_1=2E(k^2)/K(k^2)-1,$$
$$F_2=2E(k^2)/K(k^2)+2(k^2-1),$$
$$F_3=\frac{4}{3}[(2k^2-1)E(k^2)/K(k^2)+(1-k^2)], \quad (27)$$

and

$$\alpha=-\frac{2R\mu_0}{B^2}\frac{dp}{dr}q^2. \quad (28)$$

Before the dispersion relation can be solved numerically the various quantities that characterise the plasma must be defined. The profile of $\Omega_\Phi(r)$ is modelled for $r<r_1$, by

$$\Omega_\Phi(r)=\Omega_{\Phi 0}\left[1-\left(\frac{2r}{a}\right)^2\right]. \quad (29)$$

The high rotation shear within $r_1$ indicates that finite $\Omega_\Phi$ will have an important effect on the stability of the internal kink mode. The sign of $\Omega_\Phi$ is also crucial. If $\Omega_\Phi>0$, then $\Omega_\Phi$ and $\omega_{*pi}$ are in the same direction. Henceforth, $\Omega_\Phi>0$ is referred to as co-rotation and $\Omega_\Phi<0$ as counter-rotation.

In Section 4 $\hat{\Omega}_\Phi$, where

$$\hat{\Omega}_\Phi\equiv\frac{\Omega_\Phi(r_1)}{\omega_{*pi}(r_1)}$$

is used as the independent variable and the dependent variable is $\beta_p$ or, equivalently, the central temperature $T_0$, which must necessarily satisfy the marginally stable dispersion relation. The effect of the different profiles of the density and temperature is also investigated. It is assumed that $n_i=n_{i0}[1-(r/a)^2]^{\nu_n}$ and $T_i=T_0[1-(r/a)^2]^{\nu_T}$, with

$n_i = n_e$ and $T_e = T_i$. Different values are assigned to the pressure profile index $\nu_n + \nu_T$ and the parameter $\eta_i$:

$$\eta_i \equiv \frac{d \ln T_i}{d \ln n_i} = \frac{\nu_T}{\nu_n}. \tag{30}$$

The following profiles and parameters, which are typical of JET equilibria, are used: $R_0/a = 2.4$, $B_0 = 3\mathrm{T}$, $n_{i0} = 4 \times 10^{19}$ m$^{-3}$ and $Z = 1$. The safety factor profile is $q = q_0 \left[1 + d(r/a)^{2c}\right]^{1/c}$, with $q_0 = 0.7$, $d = 9.09$, $c = 1.33$ giving $r_1/a = 0.36$ and $q(a) = 5$.

For this equilibrium the coefficients, $\delta\hat{W}_n$, in Eq.(19) take the values $\delta\hat{W}_0 = 0.027$, $\delta\hat{W}_1 = 0.133$ and $\delta\hat{W}_2 = 0.359$. The equilibrium is therefore unstable according to the Bussac stability criterion (inequality (19) with $\mu_1 = 0$) for $\beta_p > 0.15$. The addition of trapped ion compression in the Kruskal-Oberman form (inequality (19) with $\mu_1 = 1.1$) raises this beta limit to $\beta_p \approx 0.19$ (when $\nu_n + \nu_T = 3$) and to $\beta_p = 0.25$ (when $\nu_n + \nu_T = 3/2$). In the next section we evaluate the effect on this beta limit of trapped ion drift resonance and FLR stabilisation, in the presence of sheared toroidal flow.

## 4. Results

The purpose of this section is to demonstrate the sensitivity of the internal kink mode to changes in $\hat{\Omega}_\Phi$. We first investigate the mode satisfying $\hat{\omega} > 1$ in an equilibrium with $\nu_n + \nu_T = 3$ and $\eta_i = 2$. Figure 1 (a) shows $\Re\{\delta\hat{W}_{ki}\}$, $\Im\{\delta\hat{W}_{ki}\}$ and the layer term $-\Im\{\hat{D}^s\}$ as a function of $\hat{\omega}$ for $\hat{\Omega}_\Phi = 0$ and $\beta_p = 0.26$, where we define:

$$\hat{D}^s = -i \frac{s(1+\Delta)^{1/2}}{3\pi\varepsilon^2} \frac{\sqrt{\tilde{\omega}(\tilde{\omega} - \omega_{*pi})}}{\omega_A}\bigg|_{r_1}, \tag{31}$$

such that $\hat{D}^s + \delta\hat{W} = 0$ and '$s$' denotes singular layer. The solution for $\hat{\omega}$ occurs when $\Im\{\delta\hat{W}_{ki}\} = -\Im\{\hat{D}^s\}$, i.e. when Eq. (21) is satisfied, clearly indicated in Fig. 1 (a) from which it can be seen that $\Re\{\delta\hat{W}\} < 0$. However, it should be noted that for the parameters assigned in this example, the thorn does not correspond to a self consistent solution of Eq. (22) (the real component of the dispersion relation), although Fig. 1 (a) does highlight a sharp peak and trough of $\Re\{\delta\hat{W}_{ki}\}$ and demonstrates how the solution is constructed. Figure 1 (b) is for a toroidal plasma rotation $\hat{\Omega}_\Phi = 2.5$. In contrast with the previous case the solution for $\hat{\omega}$, which corresponds to the thorn, now occurs close to a peak in $\Re\{\delta\hat{W}_{ki}\}$ rather than a trough. Consequently Fig. 1 (b) suggests that for the particular choice of equilibrium, co-rotation ($\hat{\Omega}_\Phi > 0$) provides enhanced stability. The reason for this is simple: the real and imaginary parts of $\delta\hat{W}_{ki}$ are altered by a shift in frequency $\Omega_\Phi(r) - \Omega_\Phi(r_1)$ as indicated by Eq. (17), whereas the inertia term is not affected.

The marginally stable dispersion relation is now solved self-consistently. However, we first note that a complete investigation of internal kink stability requires consideration of the effects of $\eta_i$, Eq. (30). $\eta_i$ can vary from one discharge to another,

and also can evolve during the sawtooth cycle. The values of $\eta_i$ are typical of those measured and fall in the range $1/4 \leq \eta_i \leq 4$.

Figure 2 shows three solutions to the dispersion relation, each with $\nu_T + \nu_n = 3$, for different values of $\eta_i$. Figure 2 (a) depicts the normalised self-consistent mode frequency $\hat{\omega}^c$ as a function of the normalised plasma rotation $\hat{\Omega}_\Phi$ for differing $\eta_i$. Such normalisation allows the boundary between the Alfvén continuum and the gap to be easily located in Fig. 2 (a) at $\hat{\omega}^c = 1$. Other fundamental parameter values can also be identified in Fig. 2. For example at $\hat{\Omega}_\Phi = 1$, the total plasma rotation $\Omega$ at $r_1$ has equal contributions from the pressure and electric field, whilst at $\hat{\Omega}_\Phi = -1$, the total plasma rotation is zero at $r_1$.

Since $\Re\{\delta W_{ki}\}$ is (approximately) proportional to $\beta_p$, Figs. 2 (b) and (c) appear to be similar. For each $\eta_i$, both $\beta_p^c$ and $\Re\{\delta W_{ki}\}$ are minimised for $\hat{\Omega}_\Phi \approx 0$, and the minimised value of the threshold beta corresponds to $\Re\{\delta W_{ki}\} < 0$, whereas $\beta_p^c$ and $\Re\{\delta W_{ki}\}$ are maximised for $\hat{\Omega}_\Phi \approx 2$. Within the range $-3 < \hat{\Omega}_\Phi < 0$ the threshold beta only increases slightly for increasing counter-rotation.

Figure 2 demonstrates that $\beta_p^c$ is increasingly sensitive to changes in $\hat{\Omega}_\Phi$ for larger values of $\eta_i$. This trend is enhanced when the peaking of the pressure profile is reduced. Figure 3 illustrates the modifications to Fig. 2 for when $\nu_T + \nu_n = 3/2$. It can be seen that for $\eta_i = 4$, the magnitude of $\beta_p^c$ varies by a factor of two within the range $0 < \hat{\Omega}_\Phi < 1$, and can rise to values three times greater than the Bussac value of $\beta_p^c = 0.15$ for this equilibrium.

For all but the case $\eta_i = 1/4$, Fig. 3 illustrates that counter-rotation modifies $\Re\{\delta W_{ki}\}$ and $\beta_p^c$ only slightly. However, for $\eta_i = 1/4$ with $-2.4 \lesssim \hat{\Omega}_\Phi \lesssim -0.5$, the marginal internal kink mode lies in the gap in the Alfvén continuum, i.e. $0 < \hat{\omega}^c < 1$. For $\hat{\Omega}_\Phi \lesssim -2.4$ or $\hat{\Omega}_\Phi \gtrsim -0.5$ the mode is in the continuum with, respectively, $\hat{\omega}^c < 0$ or $\hat{\omega}^c > 1$. When the marginal frequency lies in the gap, Eq. (24) shows that the inertial layer term $\Re\{\hat{D}^s\}$ contributes to the real part of the dispersion relation and has the effect of enhancing $\beta_p^c$; this represents the familiar diamagnetic stabilising effect which peaks when $\hat{\omega}^c = 1/2$, as confirmed by Fig. 3 (a) and (b).

Figures 2 and 3 demonstrate that the threshold poloidal beta is an increasingly sensitive function of $\hat{\Omega}_\Phi$ for increasing $\eta_i$. Comparisons between Figs. 2 and 3 show that the pressure profile also influences $\beta_p^c$. In particular, for a fairly flat profile ($\nu_n + \nu_T = 3/2$), $\beta_p^c$ is most sensitive to changes in $\hat{\Omega}_\Phi$ about unity, whereas for steeper pressure gradients ($\nu_n + \nu_T = 3$), larger values of $\hat{\Omega}_\Phi$ are required to produce a similar degree of sensitivity.

## 5. Summary and Discussion

In this paper the ideal internal kink stability analysis has been modified to include the effects of finite Larmor radius (FLR) stabilisation, trapped ion compression and ion Landau drift resonance in the presence of small sheared toroidal flow in the equilibrium.

The latter, which includes a component $\Omega_\Phi$ caused by the equilibrium radial electric field, is limited to an order of magnitude similar to that of the thermal ion diamagnetic frequency. The ideal internal kink mode calculations take into account the kinetic response of thermal ions in both the singular layer (close to $q = 1$) and the external region. Modifications arising from the inclusion of $\Omega_\Phi$ are shown to exist solely in the external kinetic term. If $\Omega_\Phi$ is not sheared, except for a Doppler shift in the real mode frequency, there is no effect on the internal kink mode. If $\Omega_\Phi$ is sheared, the enhancement to the total plasma rotation $\Omega = \Omega_\Phi + \omega_{*pi}$ has the effect of locally shifting $\delta W_{ki}[\tilde{\omega}]$ to $\delta W_{ki}[\tilde{\omega} + \Omega_\Phi(r_1) - \Omega_\Phi(r)]$. For modes with $\tilde{\omega} \sim \omega_{*pi} \sim \langle\omega_{mdi}\rangle$, the result of a frequency shift $\Omega_\Phi(r) - \Omega_\Phi(r_1) \sim \omega_{*pi}$ is to modify dramatically $\beta_p^c$, the beta limit for internal kink stability.

In general it is found that $\beta_p^c$ is an increasingly sensitive function of $\Omega_\Phi$ for increasing $\eta_i$. Provided $\eta_i$ is not much less than unity, counter-rotation has little effect on $\beta_p^c$, whereas co-rotation enhances $\beta_p^c$ by up to a factor of three above the fluid MHD limit (ie the value calculated by Bussac *et al* analysis). In particular, choosing a relatively flat pressure profile ($\nu_n + \nu_T = 3/2$) and large $\eta_i$, $\beta_p^c$ proves to be very sensitive to small changes in co-rotation.

This paper has demonstrated that finite $\Omega_\Phi$ has an important effect on the internal kink stability of tokamak plasmas in the banana regime. Furthermore, the results may explain some of the observed interaction between sawtooth stability and plasma rotation [11]. For further experimental interpretation the dispersion relation of Eq. (15) could easily be modified to include the effects of an NBI population. The additional term $\delta\hat{W}_{kh}(\tilde{\omega})$ would be identical to Eq. (17) except for the interchange of the thermal ion distribution function, diamagnetic frequency and precessional drift frequency with $f_h$, $\omega_{*h}$ and $\langle\omega_{mdh}\rangle$, respectively. It is plausible that in many NBI experiments the plasma rotation could be ordered such that $\Omega_\Phi(r_1) \sim \langle\omega_{mdh}\rangle$, and this being the case, the effects of finite sheared $\Omega_\Phi$ should be included when using internal kink models to interpret sawtooth and fishbone behaviour in such discharges.

## 6. Acknowledgements

We would like to thank Drs C G Gimblett, J W Connor and R O Dendy for a number of useful discussions and for commenting on the manuscript. This work was funded in part by the Engineering and Physical Sciences Research Council, the UK Department of Trade and Industry and Euratom.

## Appendix: Kinetic Modifications of the Singular Layer

This appendix calculates the leading order kinetic potential energy $\delta W_{ki}^s$ which modifies the minimised energy of the singular layer. We must first calculate the perturbed kinetic distribution function, denoted by '$h$', which takes a different form to Eq. (12) which is only valid far from $r_1$.

First we consider the quantity $J$, which is defined following Eq. (4). In low beta plasmas, MHD modes satisfy $B\nabla\cdot\boldsymbol{\xi}^s_\perp = -2B\boldsymbol{\xi}^s_\perp\cdot\boldsymbol{\kappa} = -2(\boldsymbol{\xi}^s_\perp\cdot\nabla)B$. In addition, the leading order displacement satisfies $\nabla\cdot\boldsymbol{\xi}^s_\perp = 0$, and, consequently, in the singular layer the discontinuity of the internal kink eigenfunction gives $\xi^s_\theta \gg \xi^s_r$. Using $(v_\parallel^2+\mu B)\partial B/\partial\theta = -B^2 v_\parallel \partial(v_\parallel/B)/\partial\theta$,

$$-2\mathcal{E}J = (v_\parallel^2+\mu B)\frac{\boldsymbol{\xi}^s_\perp\cdot\nabla B}{B} = -Bv_\parallel\frac{\xi^s_\theta}{r}\frac{\partial}{\partial\theta}\left(\frac{v_\parallel}{B}\right). \tag{A.1}$$

The poloidal displacement takes the form $\boldsymbol{\xi}^s_\theta = \hat{\boldsymbol{\xi}}^s_\theta(r)\exp(i\theta - i\phi - i\omega t)$ and the perturbed kinetic distribution function $h = \hat{h}(r,\theta)\exp(i\theta - i\phi - i\omega t)$. Hence, from Eq. (A.1) and using the ordering $\omega\sim\omega_{*i}(r_1)\sim\Omega_\Phi(r_1)\gg\omega_{mdi}(r_1)$, the drift kinetic equation becomes [13]:

$$\frac{v_\parallel}{Rq}\left[\frac{\partial}{\partial\theta}+i(1-q)\right]\hat{h} - i(\omega-\Omega_\Phi)\hat{h} = i(\omega-\omega_{*i}-\Omega_\Phi)\frac{\partial f_i}{\partial\mathcal{E}}\frac{\hat{\xi}^s_\theta}{r}\frac{v_\parallel}{R}\frac{\partial}{\partial\theta}(Rv_\parallel), \tag{A.2}$$

where the relation $B\partial R/\partial\theta = -R\partial B/\partial\theta$ results from the dependence of $B$ on $R$.

Since $q\approx 1$ in the singular layer, the $1-q$ term on the left hand side of Eq. (A.2) is neglected. Consistently with the treatment of the external region, the kinetic equation is expanded in orders of $\omega/(2\pi/\tau)$, where $\tau$ is the bounce time or transit time of trapped or passing ions, respectively. The leading order kinetic equation is

$$\frac{v_\parallel}{Rq}\frac{\partial\hat{h}_0}{\partial\theta} = i(\omega-\omega_{*i}-\Omega_\Phi)\frac{\partial f_i}{\partial\mathcal{E}}\frac{\hat{\xi}^s_\theta}{r}\frac{v_\parallel}{R}\frac{\partial}{\partial\theta}(Rv_\parallel)$$

with solution

$$\hat{h}_0 = i(\omega-\omega_{*i}-\Omega_\Phi)\frac{q\,\hat{\xi}^s_\theta}{r}\frac{\partial f_i}{\partial\mathcal{E}}Rv_\parallel + \overline{h}_0,$$

where $\overline{h}_0$ is independent of $\theta$.

Proceeding to the next order determines $\overline{h}_0$ through:

$$\frac{v_\parallel}{Rq}\frac{\partial\hat{h}_1}{\partial\theta} = i(\omega-\Omega_\Phi)\hat{h}_0, \tag{A.3}$$

which, in conjunction with the leading order solution, gives

$$\frac{v_\parallel}{Rq}\frac{\partial\hat{h}_1}{\partial\theta} = -(\omega-\Omega_\Phi)(\omega-\omega_{*i}-\Omega_\Phi)\frac{q\,\hat{\xi}^s_\theta}{r}\frac{\partial f_i}{\partial\mathcal{E}}Rv_\parallel + i(\omega-\Omega_\Phi)\overline{h}_0. \tag{A.4}$$

A solution for $\overline{h}_0$ is obtained by annihilating $\hat{h}_1$ separately for passing and trapped ions.

Transit averaging Eq. (A.4) over passing particle space annihilates $\hat{h}_1$ directly to give

$$\overline{h}_0(\text{pass}) = -i(\omega-\omega_{*i}-\Omega_\Phi)\frac{q\,\hat{\xi}^s_\theta}{r}\frac{\partial f_i}{\partial\mathcal{E}}\oint d\theta\, R^2 \Big/ \oint\frac{d\theta\,R}{v_\parallel}.$$

Annihilating $\hat{h}_1$ for trapped particles gives the result.

$$\overline{h}_0(\text{trap}) = 0.$$

Therefore, the leading order kinetic distribution function is

$$\hat{h}_0 = i(\omega - \omega_{*i} - \Omega_\Phi)\frac{q\,\hat{\xi}^s_\theta}{r}\frac{\partial f_i}{\partial \mathcal{E}} R v_\parallel \mathcal{X}, \tag{A.5}$$

with

$$\mathcal{X} = \begin{cases} 1 & \text{trapped ions} \\ 1 - (\oint d\theta\, R^2) \Big/ \left( R v_\parallel \oint \frac{d\theta\, R}{v_\parallel} \right) & \text{passing ions.} \end{cases}$$

It is now necessary to determine how kinetic effects in the layer modify the internal kink stability. This is achieved through evaluating $\delta W^s_{ki}$, the kinetic potential energy at the singular layer. It follows from Chen et al [3] that $\delta W^s_{ki}$ can be defined as:

$$\delta W^s_{ki} = \frac{1}{2}\int d^3x \left( \delta P^s_{\parallel ki} + \delta P^s_{\perp ki} \right) \frac{\xi^{s*}_\perp \cdot \nabla B}{B}$$

with

$$\delta P^s_{\parallel ki} + \delta P^s_{\perp ki} = m_i \int d^3v \left[ v^2_\parallel + \mu B \right] h.$$

Note that $\delta W^s_{ki}$ is non-zero when $h$ is even in $v_\parallel$, and the largest even component of $h$ is $h_1$. Hence, from Eq. (A.1)

$$\delta W^s_{ki} = -m_i 4\pi^2 R_0 B_0^2 \int_s dr \int_0^\infty d\mathcal{E}\, \mathcal{E} \int_0^{1/B_{\min}} d\lambda \oint d\theta\, \xi^{s*}_\theta h_1 \frac{\partial}{\partial \theta}\left( \frac{v_\parallel}{B} \right),$$

where the integration in $\theta$ is defined appropriately for either passing or trapped ions in conjunction with the integration over pitch angle $\lambda$. Integrating the poloidal integral by parts, and noting that $\xi^{s*}_\theta h_1 = \hat{\xi}^s_\theta \hat{h}_1$, gives

$$\delta W^s_{ki} = m_i 4\pi^2 R_0 B_0^2 \int_s dr\, \hat{\xi}^s_\theta \int_0^\infty d\mathcal{E}\, \mathcal{E} \int_0^{1/B_{\min}} d\lambda \oint d\theta \left( \frac{v_\parallel}{B} \right) \frac{\partial \hat{h}_1}{\partial \theta}.$$

Referring to Eq. (A.3), note that $\delta W^s_{ki}$ can be written in terms of the leading order distribution function $\hat{h}_0$. Hence, substituting Eq. (A.5) gives

$$\delta W^s_{ki} = -m_i \pi R_0 B_0 \gamma_I^2 \int_s dr\, \frac{(q\hat{\xi}^s_\theta)^2}{r} \oint d\theta \left( \frac{R}{B} \right)^2 \left[ 4\pi B \int_0^\infty d\mathcal{E}\, \mathcal{E} \frac{\partial f_i}{\partial \mathcal{E}} \int_0^{1/B_{\min}} d\lambda\, v_\parallel \right.$$
$$\left. - 4\,\pi \left( \frac{B}{R} \right) \int_0^\infty d\mathcal{E}\, \mathcal{E} \frac{\partial f_i}{\partial \mathcal{E}} \int_0^{1/B_{\max}} d\lambda \frac{\oint d\theta\, R^2}{\oint d\theta\, R/v_\parallel} \right], \tag{A.6}$$

where the notation $\gamma_I^2 = -(\omega - \Omega_\Phi)(\omega - \omega_{*pi} - \Omega_\Phi)|_{r_1}$ has been used.

The first term in the square brackets of Eq. (A.6) is evaluated over all particle velocity space and is identified with the ion density $n_i = \int dv^3 f_i$. The remaining term is more complicated. By transforming to a new pitch angle variable $y = 1/k^2$, it can be seen that the integral $\oint d\theta\, R/v_\parallel$ gives rise to an elliptic integral of the first kind, $K(y)$. Evaluating the energy integral with $\rho = m_i n_i$ one finds

$$\delta W^s_{ki} = 2\pi^2 R_0 \gamma_I^2 \int_s dr\, r (q\hat{\xi}^s_\theta)^2 \rho \frac{1}{\varepsilon^2} \left[ \underbrace{\int_{-\pi}^{\pi} \frac{d\theta\, R^4}{2\pi R_0^4}}_{1+3\varepsilon^2} - \underbrace{\left( \int_{-\pi}^{\pi} \frac{d\theta\, R^2}{2\pi R_0^2} \right)^2}_{1+\varepsilon^2} \mathcal{Q} \right], \tag{A.7}$$

where

$$\mathcal{Q} = \frac{3\pi}{\sqrt{2}} \int_0^1 \frac{dy\, \varepsilon^{3/2}}{[y(1-\varepsilon) + 2\varepsilon]^{5/2} K(y)}. \tag{A.8}$$

Defining $t = 2\varepsilon/(1-\varepsilon)$ and integrating (A.8) by parts, results in

$$\mathcal{Q} = -\frac{\pi}{2} \frac{1}{(1-\varepsilon)} \left( \left[ \frac{t^{3/2}}{(y+t)^{3/2} K(y)} \right]_0^1 + \mathcal{I} \right),$$

where

$$\mathcal{I} = \int_0^1 \frac{dy\, t^{3/2}\, K(y)'}{(y+t)^{3/2} K(y)^2},$$

and $' \equiv d/dy$. Since $1/K(1) = 0$ and $1/K(0) = 2/\pi$,

$$\mathcal{Q} = \frac{1}{1-\varepsilon} \left( 1 - \frac{\pi}{2} \mathcal{I} \right).$$

$\mathcal{I}$ still cannot be evaluated explicitly in terms of the parameter $t$ but an asymptotic expansion may be obtained for small $t$ by writing

$$\mathcal{I} \equiv t^{3/2} \left[ \int_0^1 \left( \frac{K(y)'}{K(y)^2} - \mathcal{S}(y) \right) \frac{dy}{(y+t)^{3/2}} + \int_0^1 \frac{dy\, \mathcal{S}(y)}{(y+t)^{3/2}} \right]. \tag{A.9}$$

Here $\mathcal{S}$ is chosen so that the second integral can be evaluated analytically in such a way that on taking $t = 0$, the first integral converges at $y = 0$. Hence $\mathcal{S}(0) = K(0)'/K(0)^2$ and its local dependence for small $y$ is obtained using the expansion

$$K(y) = \frac{\pi}{2} \left[ 1 + \frac{1}{4} y + \frac{9}{64} y^2 + ... \right].$$

Truncating $\mathcal{S}$ beyond $y^2$, we take

$$\mathcal{S} = \frac{1}{2\pi} \left[ 1 + \frac{5}{8} y \right],$$

and so the second integral of Eq. (A.9) is

$$t^{3/2} \int_0^1 \frac{dy\, \mathcal{S}(y)}{(y+t)^{3/2}} = \frac{2}{\pi} \left[ \varepsilon - \frac{3\sqrt{2}}{8} \varepsilon^{3/2} \right] + O(\varepsilon^2).$$

The first integral of Eq. (A.9) can now be evaluted numerically taking $t = 0$. Hence,

$$\mathcal{I} = \frac{2}{\pi} \left[ \varepsilon - \frac{3\sqrt{2}}{8} \varepsilon^{3/2} + (2\varepsilon)^{3/2} \int_0^1 \left( \frac{K(y)'}{K(y)^2} - \mathcal{S}(y) \right) \frac{dy}{y^{3/2}} \right] + O(\varepsilon^2)$$

or, on numerical evaluation,

$$\mathcal{I} = \frac{2}{\pi} \left[ \varepsilon + 1.6\varepsilon^{3/2} \right] + O(\varepsilon^2).$$

The terms in $\mathcal{Q}$ of order $\varepsilon$ now cancel to leave :

$$\mathcal{Q} = 1 - 1.6\varepsilon^{3/2} + \mathcal{Q}_2 \varepsilon^2,$$

where evaluation of $\mathcal{Q}_2$ requires a higher order construction of $S(\mathcal{I})$ above. Upon substituting $\mathcal{Q}$ into Eq. (A.7), the leading order terms cancel to give

$$\delta W_{ki}^s = 2\pi^2 R_0 \gamma_I^2 \int_s dr\, r (q \hat{\xi}_\theta^s)^2 \rho \Delta, \tag{A.10}$$

with

$$\Delta = \left( \frac{1.6}{\varepsilon_1^{1/2}} + 2 - \mathcal{Q}_2 \right) q^2.$$

Equation (A.10) is easily combined with the fluid contributions to the dispersion relation and, following the procedure described in Refs. [15, 16], yields the dispersion relation of Eq. (13). The leading order term of $\Delta$ is $1.6/\varepsilon_1^{1/2}$, and represents a correction to the inertial enhancement calculated by Mikhailovskii and Tyspin [19]. The term +2 is also observed in collisional MHD where it appears as an enhancement from the parallel inertia [17]. The remaining term, $Q_2$, can be evaluted by a similar procedure, and has the value 1.5, so that, finally,

$$\Delta = \left[ \frac{1.6}{\epsilon_1^{1/2}} + 0.5 + O(\epsilon_1^{1/2}) \right] q^2.$$

## References


[1] K. McGuire *et al*, Phys. Rev. Lett. **50**, 891 (1983).
[2] S. von Goeler, W. Stodiek and N. Sauthoff, Phys. Rev. Lett. **33**, 1201 (1974).
[3] L. Chen, R. B. White and M. N. Rosenbluth, Phys. Rev. Lett. **52**, 1122 (1984).
[4] M. N. Bussac, R. Pellat, D. Edery and J. L. Soulé, Phys. Rev. Lett. **35**, 1638 (1975).
[5] D. J. Campbell *et al*, Phys. Rev. Lett. **60** 2148 (1988).
[6] J. P. Graves, K. I. Hopcraft, R. O. Dendy, R. J. Hastie, K. G. McClements and M. Mantsinen, Phys. Rev. Lett. **84**, 1204 (2000).
[7] J. P. Graves, Ph.D. Thesis, University of Nottingham (1999).
[8] G. Fogaccia and F. Romanelli, Phys. Plasmas **2**, 227 (1994).
[9] T. M. Antonsen Jr. and A Bondeson, Phys. Rev. Lett. **71**, 2046 (1993).
[10] H. J. de Blank, 17th Euro. Proc. Phys. Soc. Conf. (Cont. Fus. and Plas. Phys.) **2**, 919 (1990).
[11] T. C. Hender, R. Fitzpatrick, A. W. Morris, P. G. Carolan, R. D. Durst, *et al*, Nucl. Fusion **32**, 2091 (1992).
[12] J. W. Connor, S. C. Cowley, R. J. Hastie and L. R. Pan, Plasma Phys and Control Fusion **29**, 919 (1987).
[13] T. M. Antonsen and Y. C. Lee, Phys. Fluids **25**, 142 (1982).
[14] M. N. Rosenbluth and M. L. Sloan, Phys. Fluids **14**, 1725 (1971).
[15] M. N. Bussac, D. Edery, R. Pellat and J. L. Soule, in Plasma Phys. and Controlled Nucl. Fusion Research 1976 (IAEA, Vienna 1977), Vol. 1, p607.
[16] G. Ara, B. Basu, B. Coppi, G. Laval, M. N. Rosenbluth and B. V. Waddell, Annals of Physics **112**, 443 (1978).
[17] A. H. Glasser, J. M. Green and J. L. Johnson, Phys. Fluids **18**, 875 (1975).
[18] T. M. Antonsen, in *Theory of Fusion Plasmas* (eds A. Bondeson, E. Sindoni and F. Troyon), Editrice Compositori Bologna, Varenna (1987), p. 161.
[19] A. B. Mikhailovskii and V. S. Tsypin, Sov J . Plasma Phys. **9**, 91 (1983).
[20] M. Abramowitz and I. A. Stegun *Handbook of Mathematical Functions*. Dover Publications, Inc, New York (1965).
[21] M. D. Kruskal and C. R. Oberman, Phys. Fluids **1**, 275 (1958).
[22] J. W. Connor, R. J. Hastie and T. J. Martin, Nucl. Fusion **23**, 1702 (1983).
[23] T. S. Taylor E. J. Strait, L. L. Lao, M. Mauel, A. D. Turnbull, *et al*, Phys. Plasmas **2**, 2390 (1995).

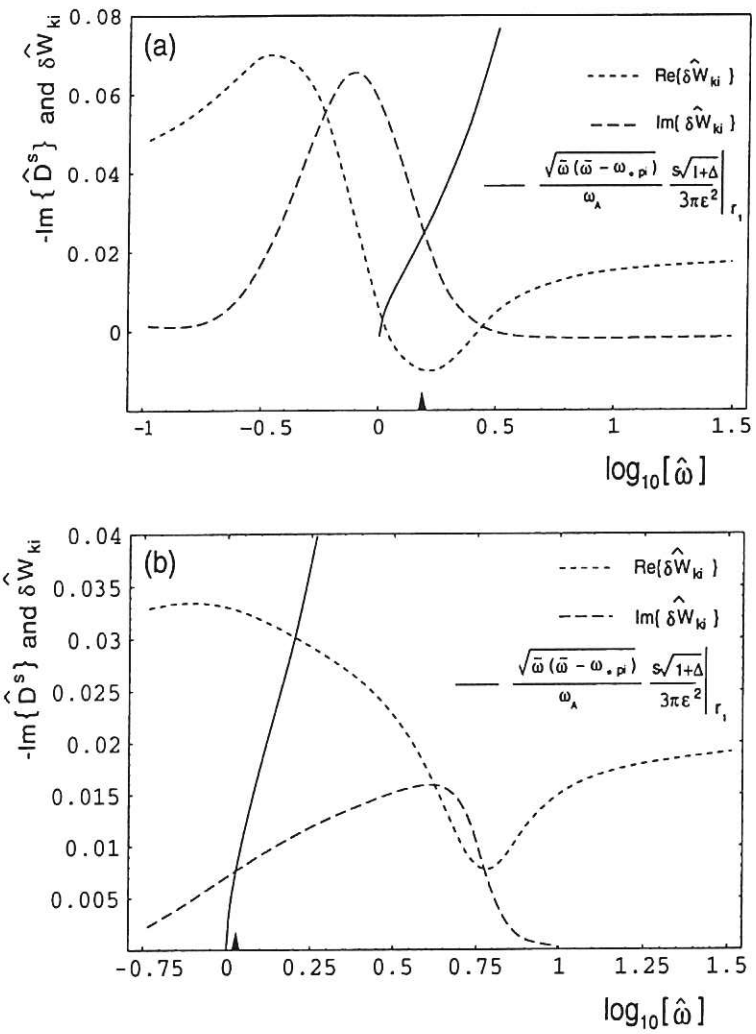


**Figure 1.** Plots of real and imaginary kinetic potential energy terms together with the singular layer term $\hat{D}^s$ as a function of the normalised mode frequency $\hat{\omega} \equiv \tilde{\omega}/\omega_{*pi}(r_1)$ for an equilibrium with $\nu_n + \nu_T = 3$, $\eta_i = 2$ and $\beta_p = 0.25$. In (a) the plasma rotation $\hat{\Omega}_\Phi = 0$ and in (b) $\hat{\Omega}_\Phi = 2.5$. The solutions to the imaginary component of dispersion relation (Eq. (21)) occur for values of $\hat{\omega}$ corresponding to the thorns.

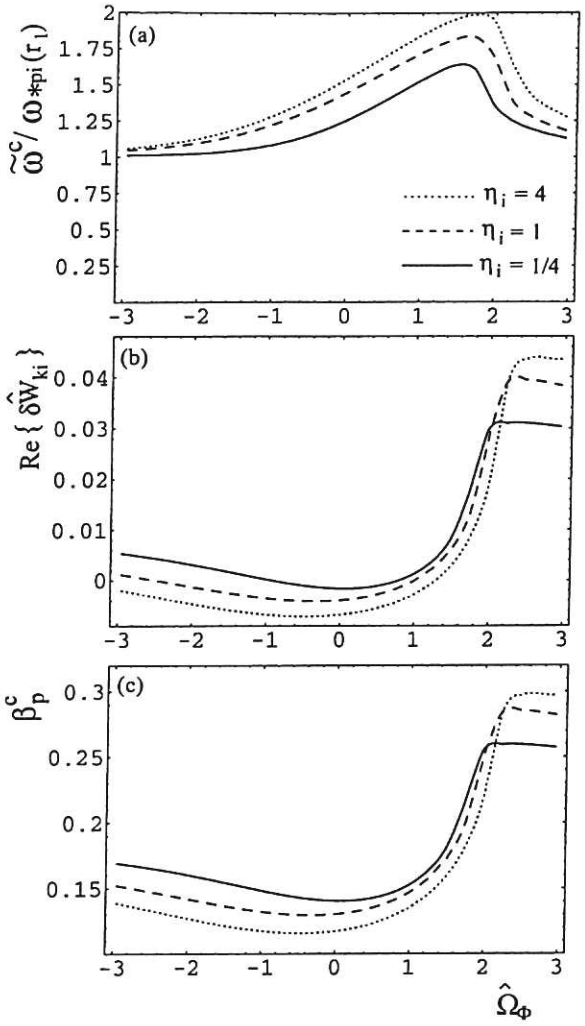


**Figure 2.** Depicting $\hat{\omega}^c \equiv \tilde{\omega}^c/\omega_{*pi}(r_1)$, $\Re\{\delta\hat{W}_{ki}\}$ and $\beta_p^c$ as a function of $\hat{\Omega}_\Phi$ for three different values of $\eta_i$. In each plot the pressure profile is parameterised by $\nu_T + \nu_n = 3$.

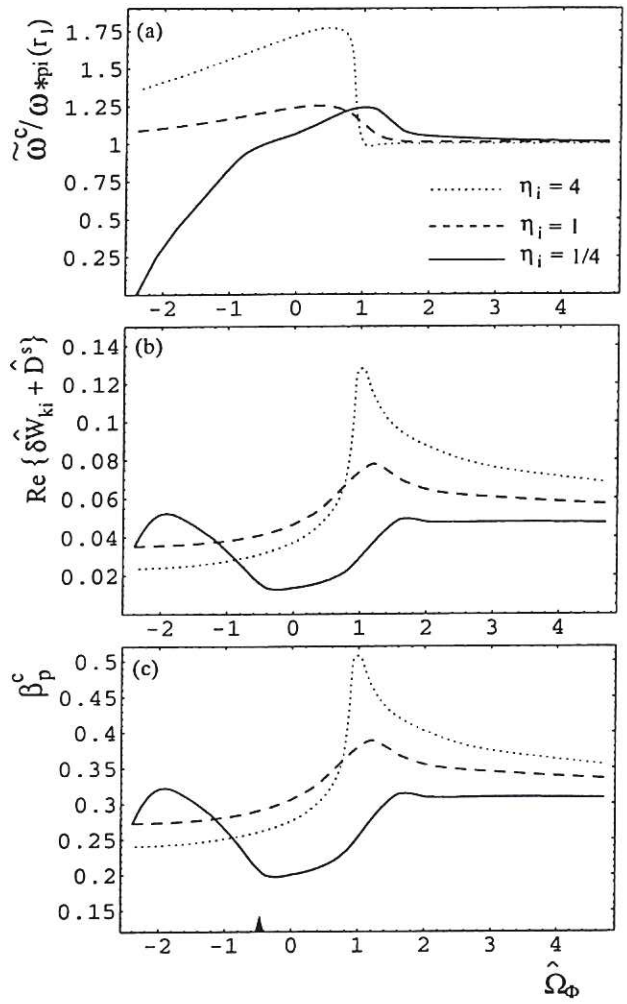


**Figure 3.** Depicting $\hat{\omega}^c \equiv \tilde{\omega}^c/\omega_{*pi}(r_1)$, $\Re\{\delta\hat{W}_{ki} + \hat{D}^s\}$ and $\beta_p^c$ as a function of $\hat{\Omega}_\Phi$ for three different values of $\eta_i$. In each plot the pressure profile is parameterised by $\nu_T + \nu_n = 3/2$. Note that $\Re\{\hat{D}^s\} = 0$ for modes in the continuum. The thorn indicates the frequency transition as the marginal mode moves out of the gap into the continuum for $\eta_i = 1/4$.